

Learned Half-Quadratic Splitting Network for Magnetic Resonance Image Reconstruction

Bingyu Xin¹

bx64@RUTGERS.EDU

Timothy S. Phan²

TIMOTHY.S.PHAN@NYULANGONE.ORG

Leon Axel²

LEON.AXEL@NYULANGONE.ORG

Dimitris N. Metaxas¹

DNM@CS.RUTGERS.EDU

¹ Department of Computer Science, Rutgers University, Piscataway, NJ 08854, USA.

² Department of Radiology, New York University, New York, NY 10016, USA.

Editors: Under Review for MIDL 2022

Abstract

Magnetic Resonance (MR) image reconstruction from highly undersampled k -space data is critical in accelerated MR imaging (MRI) techniques. In recent years, deep learning-based methods have shown great potential in this task. This paper proposes a learned half-quadratic splitting algorithm for MR image reconstruction and implements the algorithm in an unrolled deep learning network architecture. We compare the performance of our proposed method on a public cardiac MR dataset against DC-CNN and LPDNet, and our method outperforms other methods in both quantitative results and qualitative results with fewer model parameters and faster reconstruction speed. Finally, we enlarge our model to achieve superior reconstruction quality, and the improvement is 1.76 dB and 2.74 dB over LPDNet in peak signal-to-noise ratio on 5 \times and 10 \times acceleration, respectively. Code for our method is publicly available at <https://github.com/hellopipu/HQS-Net>.

Keywords: MR reconstruction, k -space, Compressed sensing, Deep Learning, Cardiac

1. Introduction

Magnetic resonance imaging (MRI) has been widely used in clinical disease diagnosis as a non-invasive imaging technique with a high spatio-temporal signal-to-noise ratio (SNR). However, the main limitation for MRI is the slow acquisition procedure, which usually lasts between 15 to 90 minutes per subject. For dynamic cardiac MRI, subjects are required to hold their breath and stay still to reduce imaging artifacts during the acquisition process, which is challenging or even impossible for those with breathing difficulties.

In MRI physics, k -space is the 2D or 3D Fourier transform of the MR image, and MR raw data is acquired in k -space. The recent fast MRI techniques aim to reduce the MRI acquisition time by scanning undersampled k -space data, which are then used to reconstruct the MR images by applying an inverse Fourier transform. This data undersampling process violates the Nyquist Theorem, and therefore the reconstructed images will be heavily aliased, which will result in imaging artifacts and low SNR.

Traditional compressed sensing MR image reconstruction methods (Ma et al., 2008) (Ravishankar and Bresler, 2010) (Boyd et al., 2011) (Lingala et al., 2011) are time-consuming, and the reconstruction quality is often not satisfactory. The recent use of deep learning methods for MR image reconstruction has resulted in improved reconstruction quality, higher SNR with significant efficiency gains at runtime.

In this work, we propose a deep learning method that is motivated by the half-quadratic splitting (HQS) algorithm (Geman and Yang, 1995) for compressed sensing MR image reconstruction. We train, validate, and test our approach on a publicly available cardiac MR dataset with a single-coil acquisition setting. We compare our method with two mainstream and high-performance methods (Schlemper et al., 2017) (Adler and Öktem, 2018) with acceleration factors of $5\times$ and $10\times$. The results demonstrate the improvements offered by our method in terms of the MR reconstruction image quality, the model size, and the efficient inference speed. We also provide a larger size model for improved image reconstruction quality.

2. Brief Literature Review

Over the past 15 years, compressed sensing (CS) methods for MR image reconstruction (Lustig et al., 2007) have been one of the most successful reconstruction methods by exploring the sparsity of the image using sparse transforms such as the wavelet transform. CS reconstructs MR images by iteratively increasing the sparsity in transform space and updating the denoised images. The Learned Iterative Shrinkage-Thresholding Algorithm (LISTA) (Gregor and LeCun, 2010) is a fast algorithm that approximates optimal sparse codes by replacing two pre-computed matrices in classical ISTA with learned ones. Based on CS, DLMRI (Ravishankar and Bresler, 2010) exploits adaptive patch-based dictionaries as a more sparse transform to improve the reconstruction performance. The Alternating Direction Method of Multipliers (ADMM) (Boyd et al., 2011) is an efficient variable splitting algorithm that decouples the CS-based MRI optimization problem into simpler subproblems.

Recently, the success of deep learning has further inspired research in MRI reconstruction (Wang et al., 2021). CNNs automatically extract features that have significantly better representational power compared to hand-crafted features used by conventional methods. Deep ADMM-Net (Sun et al., 2016) proposes a deep learnable architecture inspired by the ADMM iterative procedure for optimizing a CS MRI model. Schlemper et al. (2017) follows the iterative algorithm in DLMRI but replaces the dictionary learning reconstruction with a deep cascade of CNNs (DC-CNN). DC-CNN outperforms the conventional method significantly in both reconstruction quality and inference time and is a great baseline for today’s k -space reconstruction research. KIKI-Net (Eo et al., 2018) is a cross-domain CNN that consists of a deep CNN to process k -space data, a deep CNN to process image domain data, and an interleaved data consistency operation. MoDL (Aggarwal et al., 2018) uses an architecture involving numerical optimization blocks within the deep unrolled network with shared weights, which allows the easy use of complex forward models and additional image priors. ISTA-Net (Zhang and Ghanem, 2018) is proposed by mapping the traditional ISTA for optimizing a general l_1 norm CS reconstruction model into a deep network and can be essentially viewed as a significant extension of LISTA (Gregor and LeCun, 2010). LPDNet (Adler and Öktem, 2018) is also an iterative reconstruction scheme. It is inspired by Primal-Dual Hybrid Gradient (PDHG) algorithm (Sidky et al., 2012) where the proximal operators are replaced by learned CNNs. LPDNet was originally proposed for tomographic data reconstruction, but it shows superior performance over other methods on recent MR reconstruction challenges (Muckley et al., 2021).

In addition to the several unrolled iterative methods introduced above, some other techniques employ Generative Adversarial Networks (GANs) (Goodfellow et al., 2014) and Recurrent Neural Networks (RNNs). DAGAN (Yang et al., 2017) uses conditional GAN with several task-specific losses to reconstruct MR images. RefineGAN (Quan et al., 2018) uses a chained generator with cyclic data consistency loss to generate MR images. KIGAN (Shaul et al., 2020) uses a cascade of a k -space U-net and an image-space U-net as the generator in GAN for reconstruction. Qin et al. (2018) jointly exploits the dependencies of the temporal sequences and the iterative nature of the traditional optimization algorithms. The proposed architecture uses bidirectional RNN across time sequences to learn the spatio-temporal dependencies.

3. Proposed Method

3.1. Problem Formulation

We want to reconstruct the complex-valued MR image x from undersampled measurements y in k -space, such that:

$$y = F_u x + \epsilon \quad (1)$$

where $F_u = M F$, where M is an undersampling mask in k -space, F is the Fourier transform, ϵ is the acquisition noise. Eq.(1) is underdetermined, and hence the inversion is ill-posed. According to CS theory, we can estimate x by formulating an optimization problem:

$$\min_x \frac{1}{2} \|y - F_u x\|_2^2 + \lambda R(x) \quad (2)$$

where $\|y - F_u x\|_2^2$ is the data fidelity term, $R(x)$ is a regularization term on x and λ is to adjust the regularization based on the noise level of y . For traditional CS-based methods, the regularization term $R(x)$ typically involves l_0 or l_1 norms in the sparse domain of x .

3.2. Half Quadratic Splitting (HQS) Algorithm

The variable splitting technique is usually adopted to decouple the fidelity term and regularization term (Geman and Yang, 1995) (Boyd et al., 2011). By introducing an auxiliary variable z , Eq.(2) is equivalent to the constrained optimization problem below:

$$\min_x \frac{1}{2} \|y - F_u x\|_2^2 + \lambda R(z), \quad \text{s.t.} \quad z = x \quad (3)$$

The HQS method(Geman and Yang, 1995) solves the following problem:

$$\min_{x,z} \frac{1}{2} \|y - F_u x\|_2^2 + \lambda R(z) + \frac{\mu}{2} \|z - x\|_2^2 \quad (4)$$

where μ is a penalty parameter. Eq.(4) can be solved in an iterative strategy, HQS optimizes $\{x, z\}$ in an alternating fashion by solving the following two subproblems separately:

$$x_{k+1} = \arg \min_x \|y - F_u x\|_2^2 + \mu \|x - z_k\|_2^2 \quad (5a)$$

$$z_{k+1} = \arg \min_z \frac{\mu}{2} \|z - x_{k+1}\|_2^2 + \lambda R(z) \quad (5b)$$

The fidelity term and regularization term are decoupled into Eq.(5a) and Eq.(5b), respectively. Eq.(5a) contains the fidelity term associated with a quadratic regularized least-squares problem, and the closed-form solution is given by:

$$x_{k+1} = (F_u^H F_u + \mu I)^{-1} (F_u^H y + \mu z_k) = z_k + \frac{1}{1 + \mu} F_u^H (M y - F_u z_k) \quad (6)$$

where F_u^H is the Hermitian of F_u , I is the identity matrix. Eq.(5a) can be easily solved by Eq.(6). However, solving Eq.(5b) efficiently and effectively is non-trivial.

3.3. Learned HQS

Our goal is to derive a learned reconstruction scheme inspired by HQS. Motivated by former works (Sun et al., 2016)(Schlemper et al., 2017)(Adler and Öktem, 2018), our approach replaces Eq.(5b) by a parametrized CNN learned from training data. To allow the algorithm to utilize memory between iterations, we also use a buffer design used in (Adler and Öktem, 2018). Our proposed method is outlined in Algorithm 1.

Figure 1 shows an overview of our proposed unrolled network architecture to solve the MR reconstruction problem. The input to the network is the buffer data f_0 , which is the concatenation of m copies of the complex-valued zero-filled image x_0 , while the channel size of f_0 is $2m$. The proposed network consists of n reconstruction blocks, which correspond to n iterations in the HQS algorithm. In each reconstruction block, the first data $f_{i-1}^{(1)}$ in f_{i-1} is used for updating Eq.(5a) by the solution given in Eq.(6) denoted as an update operation in the figure. The updated $f_{i-1}^{(1)}$ will be concatenated with f_{i-1} as the input for updating Eq.(5b), while the updating module for Eq.(5b) is a learnable CNN with 3 convolutional layers denoted as red and green arrows shown in the block. Deep residual learning (He et al., 2016) is adapted in the block for better learning performance. The output of the network $f_n^{(1)}$ is the final reconstructed MR image by our method.

Algorithm 1: Learned Half-Quadratic Splitting

Input: zero-filled MR image x_0 , sampling mask M , iterations n , buffer size m
Output: reconstructed image $f_n^{(1)}$
 Initialize $f_0 = [x_0, \dots, x_0]_m$, μ and Γ_{θ_i} are learnable parameters
for $i = 1$ **to** n **do**

$$\left| \begin{array}{l} x_i \leftarrow z_{i-1} + \frac{1}{1+\mu} F_u^H (M y - F_u z_{i-1}); \\ f_i \leftarrow \Gamma_{\theta_i}(f_{i-1}, x_i); \end{array} \right.$$
end

3.4. Loss function

Following Zhao et al. (2016) and Pezzotti et al. (2020), we deploy a compound loss of MS-SSIM (Wang et al., 2003) loss and L1 loss in training:

$$\mathcal{L} = \gamma \mathcal{L}^{\text{MS-SSIM}}(x_{rec}, x_{gt}) + (1 - \gamma) \|x_{rec} - x_{gt}\|_1 \quad (8)$$

where $\mathcal{L}^{\text{MS-SSIM}}$ is MS-SSIM loss, x_{rec} is the reconstructed image, x_{gt} is the ground truth image, γ is the weight for MS-SSIM loss.

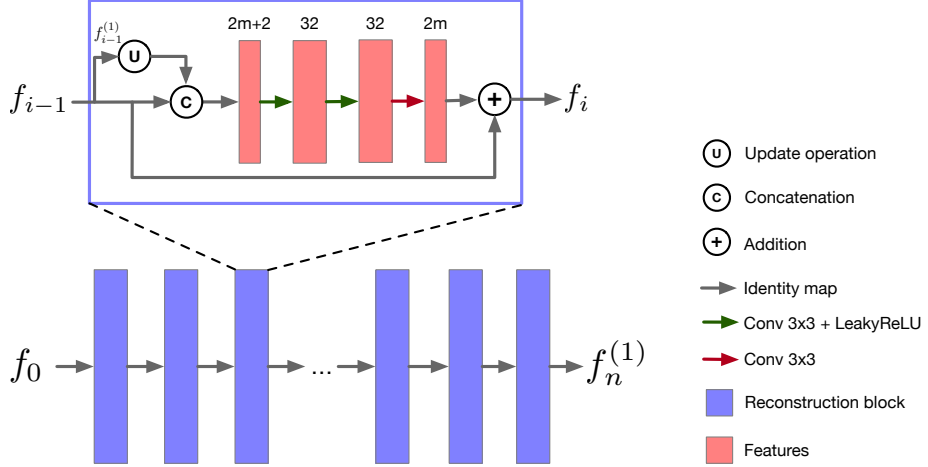


Figure 1: Overview of the proposed reconstruction network architecture. The input data f_0 is the concatenation of m copies of the complex-valued zero-filled images x_0 , the network contains n reconstruction blocks, and the final reconstructed image is $f_n^{(1)}$. In each block, the update operation is utilized by Eq.(6), a learnable CNN with three convolutional layers denoted as red and green arrows is used for updating Eq.(5b). The numbers in the figure denote the channels of the output features of the CNN layers. Skip connection is adapted for better learning performance.

4. Experiments

4.1. Dataset

We use an open-access complex-valued Cardiovascular MR (OCMR) dataset¹ (Chen et al., 2020) in our experiments. The dataset provides multi-coil k -space data from 74 fully sampled cardiac cine series. In this paper, we only experiment on 2D image slices with a single-coil setting. We first generate the emulated single-coil k -space data from the OCMR dataset using the method described in Tygert and Zbontar (2020). Each 2D image slice is processed to the size of [2,192,160], where the first dimension stores the real part and the imaginary part of the complex value. The train, validation, and test sets have 1874, 544, and 1104 slices, respectively, from a disjoint set of subjects.

4.2. Metrics

In this work, we use three commonly used metrics in the MR reconstruction task: normalized root-mean-square error (NRMSE), peak signal-to-noise ratio (PSNR), and the structural similarity index measure (SSIM) to evaluate the reconstruction quality of different methods. These metrics are computed against the fully sampled MR images. A good reconstruction will have low NRMSE, high PSNR and SSIM values.

1. <https://ocmr.info/>

Table 1: Results of different methods on two acceleration factors. The best and second best results are highlighted in **red** and **blue** colors

Acceleration factor	Metric	Zero-Filled	DC-CNN	LPDNet	Proposed	Proposed*
5×	NRMSE(%)	41.49	20.41	17.47	16.56	14.29
	PSNR(dB)	25.20	31.46	32.82	33.30	34.58
	SSIM	0.692	0.890	0.913	0.922	0.937
10×	NRMSE(%)	59.50	35.21	31.58	30.06	23.16
	PSNR(dB)	22.05	26.65	27.61	28.05	30.35
	SSIM	0.575	0.757	0.791	0.809	0.864

4.3. Experiment settings

We implemented two versions of our method in the experiments; one model is the same as shown in Figure 1, denoted as *Proposed*, while the other model is much larger, which replaces the regular CNN with a modified U-net (Zhang et al., 2021) that is shared between different reconstruction blocks, denoted as *Proposed**. We use this model to get the best reconstruction quality without considering the model size. We compare our method against two published methods, DC-CNN (Schlemper et al., 2017) and LPDNet (Adler and Öktem, 2018). We use the D5C5 version of DC-CNN. For LPDNet and two versions of our proposed method, the number of iterations n and buffer size m is set to 10 and 5, respectively. All models are trained from scratch for two different acceleration factors of 5× and 10×. We use random cartesian sampling masks throughout training and a fixed cartesian mask when validating and testing. Input data is the zero-filled image normalized to [0,1], and we apply random crop and random affine transformation as data augmentation. We use Adam optimizer, compound loss ($\gamma = 0.84$), and the learning rate is set to 0.001 for all models.

5. Results and Discussion

Quantitative Results Quantitative results of different models are summarized in Table 1. As a widely used baseline model in MR reconstruction, the reconstructed images using DC-CNN far surpass the zero-filled images of the NRMSE, PSNR, and SSIM values. LPDNet achieves better results than DC-CNN by updating reconstruction iteratively in both image and k -space domain. Our proposed model outperforms both methods in all metrics, which shows its effectiveness, and the proposed* model further improves the reconstruction quality owing to its larger model capacity. Compared to LPDNet, on 5× acceleration, the proposed* method improves the PSNR by 1.76 dB, improves the SSIM by 0.024, and reduces the NRMSE by 3.18%; on 10× acceleration, the proposed* method improves the PSNR by 2.74 dB, improves the SSIM by 0.073, and reduces the NRMSE by 8.42%.

Qualitative Results Figure 2 shows reconstructed MR image samples in the test set of different models on acceleration factors of 5× and 10×. On 5× acceleration, the zero-filled image is corrupted aliasing artifacts. The reconstructed images by different models are much better than the zero-filled image and visually similar to the ground truth. However,

we can still find subtle differences using the zoomed area and error maps. Our proposed two models get slightly better quality than the other two methods; on $10\times$ acceleration, the aliasing artifact in the zero-filled image becomes more prominent. DC-CNN and LPDNet also only generate unsatisfied recoveries. The proposed method is slightly better. The proposed* method is much better, especially in the zoomed area where the reconstructed myocardium wall and the boundary are more precise and closer to the ground truth.

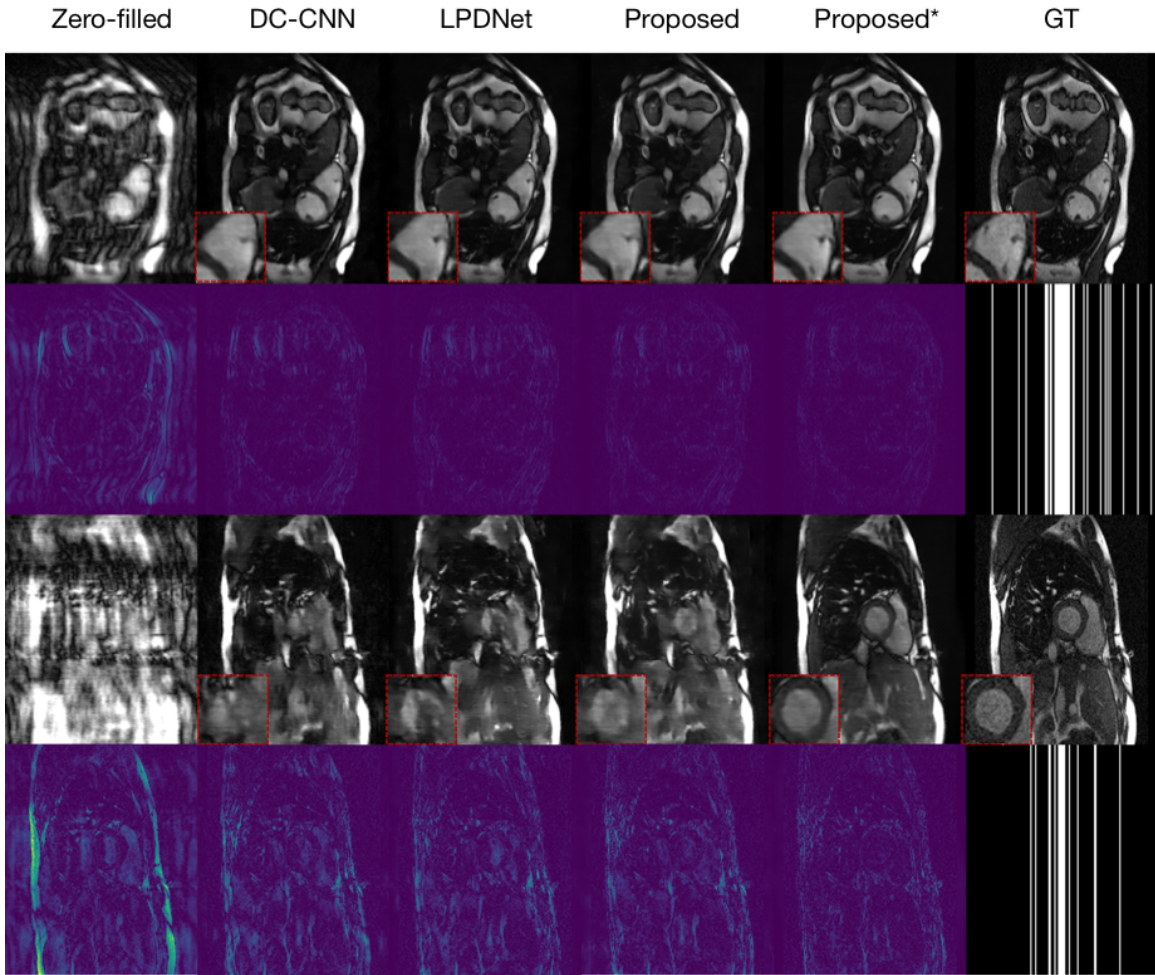


Figure 2: Reconstruction samples. The first two rows and the last two rows show the reconstructed images and error maps on the acceleration factors of $5\times$ and $10\times$, respectively. The first five columns show the reconstruction and corresponding error maps of different models, from left to right is zero-filled, DC-CNN, LPDNet, our proposed model, and proposed* model. The red square on the bottom left in each reconstructed image shows the zoomed area. The last column shows the ground truth (GT) images and the cartesian sampling masks.

Table 2: Comparison of inference time per slice and model size for different models. The best and second best results are highlighted in **red** and **blue** colors

Models	DC-CNN	LPDNet	Proposed	proposed*
time(μ s)	11.79	14.61	11.50	71.79
# of param (M)	0.54	0.30	0.15	31.14

Model Comparison Table 2 gives a summary of the number of model parameters and inference speed of these methods. Compared to the other two methods, our proposed model can achieve faster inference speeds with fewer model parameters. The proposed* model with a larger capacity can reconstruct images of much higher quality at the cost of model size and inference time. It’s worth noting that we can easily balance between the model size and reconstruction quality by choosing an appropriate buffer size m , the number of iterations n , the number of convolution layers in each reconstruction block, and the convolution channel size. We can further improve the reconstruction quality of the proposed* model by increasing these hyper-parameters.

6. Conclusion

This paper proposed a learned HQS method for MR image reconstruction. Our method outperforms other reconstruction methods with higher reconstruction quality, fewer model parameters, and faster speed. We also provide a more extensive version model to achieve visually more pleasing reconstruction results. We validate the effectiveness of our method on a public cardiac MR dataset. In future research, we will extend our approach to dynamic cardiac MR data acquired with multi-coil and radial sampling masks, which is a more realistic scenario.

References

Jonas Adler and Ozan Öktem. Learned primal-dual reconstruction. *IEEE transactions on medical imaging*, 37(6):1322–1332, 2018.

Hemant K Aggarwal, Merry P Mani, and Mathews Jacob. Modl: Model-based deep learning architecture for inverse problems. *IEEE transactions on medical imaging*, 38(2):394–405, 2018.

Stephen Boyd, Neal Parikh, and Eric Chu. *Distributed optimization and statistical learning via the alternating direction method of multipliers*. Now Publishers Inc, 2011.

Chong Chen, Yingmin Liu, Philip Schniter, Matthew Tong, Karolina Zareba, Orlando Simonetti, Lee Potter, and Rizwan Ahmad. Ocmr (v1. 0)—open-access multi-coil k-space dataset for cardiovascular magnetic resonance imaging. *arXiv preprint arXiv:2008.03410*, 2020.

Taejoon Eo, Yohan Jun, Taeseong Kim, Jinseong Jang, Ho-Joon Lee, and Dosik Hwang. Kiki-net: cross-domain convolutional neural networks for reconstructing undersampled magnetic resonance images. *Magnetic resonance in medicine*, 80(5):2188–2201, 2018.

Donald Geman and Chengda Yang. Nonlinear image recovery with half-quadratic regularization. *IEEE transactions on Image Processing*, 4(7):932–946, 1995.

Ian Goodfellow, Jean Pouget-Abadie, Mehdi Mirza, Bing Xu, David Warde-Farley, Sherjil Ozair, Aaron Courville, and Yoshua Bengio. Generative adversarial nets. *Advances in neural information processing systems*, 27, 2014.

Karol Gregor and Yann LeCun. Learning fast approximations of sparse coding. In *Proceedings of the 27th international conference on international conference on machine learning*, pages 399–406, 2010.

Kaiming He, Xiangyu Zhang, Shaoqing Ren, and Jian Sun. Deep residual learning for image recognition. In *Proceedings of the IEEE conference on computer vision and pattern recognition*, pages 770–778, 2016.

Sajan Goud Lingala, Yue Hu, Edward DiBella, and Mathews Jacob. Accelerated dynamic mri exploiting sparsity and low-rank structure: kt slr. *IEEE transactions on medical imaging*, 30(5):1042–1054, 2011.

Michael Lustig, David Donoho, and John M Pauly. Sparse mri: The application of compressed sensing for rapid mr imaging. *Magnetic Resonance in Medicine: An Official Journal of the International Society for Magnetic Resonance in Medicine*, 58(6):1182–1195, 2007.

Shiqian Ma, Wotao Yin, Yin Zhang, and Amit Chakraborty. An efficient algorithm for compressed mr imaging using total variation and wavelets. In *2008 IEEE Conference on Computer Vision and Pattern Recognition*, pages 1–8. IEEE, 2008.

Matthew J Muckley, Bruno Riemenschneider, Alireza Radmanesh, Sunwoo Kim, Geunu Jeong, Jingyu Ko, Yohan Jun, Hyungseob Shin, Dosik Hwang, Mahmoud Mostapha, et al. Results of the 2020 fastmri challenge for machine learning mr image reconstruction. *IEEE transactions on medical imaging*, 40(9):2306–2317, 2021.

Nicola Pezzotti, Sahar Yousefi, Mohamed S Elmahdy, Jeroen Hendrikus Fransiscus Van Gemert, Christophe Schuelke, Mariya Doneva, Tim Nielsen, Sergey Kastryulin, Boudewijn PF Lelieveldt, Matthias JP Van Osch, et al. An adaptive intelligence algorithm for undersampled knee mri reconstruction. *IEEE Access*, 8:204825–204838, 2020.

Chen Qin, Jo Schlemper, Jose Caballero, Anthony N Price, Joseph V Hajnal, and Daniel Rueckert. Convolutional recurrent neural networks for dynamic mr image reconstruction. *IEEE transactions on medical imaging*, 38(1):280–290, 2018.

Tran Minh Quan, Thanh Nguyen-Duc, and Won-Ki Jeong. Compressed sensing mri reconstruction using a generative adversarial network with a cyclic loss. *IEEE transactions on medical imaging*, 37(6):1488–1497, 2018.

Saiprasad Ravishankar and Yoram Bresler. Mr image reconstruction from highly undersampled k-space data by dictionary learning. *IEEE transactions on medical imaging*, 30(5):1028–1041, 2010.

Jo Schlemper, Jose Caballero, Joseph V Hajnal, Anthony N Price, and Daniel Rueckert. A deep cascade of convolutional neural networks for dynamic mr image reconstruction. *IEEE transactions on Medical Imaging*, 37(2):491–503, 2017.

Roy Shaul, Itamar David, Ohad Shitrit, and Tammy Riklin Raviv. Subsampled brain mri reconstruction by generative adversarial neural networks. *Medical Image Analysis*, 65: 101747, 2020.

Emil Y Sidky, Jakob H Jørgensen, and Xiaochuan Pan. Convex optimization problem prototyping for image reconstruction in computed tomography with the chambolle–pock algorithm. *Physics in Medicine & Biology*, 57(10):3065, 2012.

Jian Sun, Huibin Li, Zongben Xu, et al. Deep admm-net for compressive sensing mri. *Advances in neural information processing systems*, 29, 2016.

Mark Tygert and Jure Zbontar. Simulating single-coil mri from the responses of multiple coils. *Communications in Applied Mathematics and Computational Science*, 15(2):115–127, 2020.

Shanshan Wang, Taohui Xiao, Qiegen Liu, and Hairong Zheng. Deep learning for fast mr imaging: a review for learning reconstruction from incomplete k-space data. *Biomedical Signal Processing and Control*, 68:102579, 2021.

Zhou Wang, Eero P Simoncelli, and Alan C Bovik. Multiscale structural similarity for image quality assessment. In *The Thirty-Seventh Asilomar Conference on Signals, Systems & Computers, 2003*, volume 2, pages 1398–1402. Ieee, 2003.

Guang Yang, Simiao Yu, Hao Dong, Greg Slabaugh, Pier Luigi Dragotti, Xujiang Ye, Fangde Liu, Simon Arridge, Jennifer Keegan, Yike Guo, et al. Dagan: Deep de-aliasing generative adversarial networks for fast compressed sensing mri reconstruction. *IEEE transactions on medical imaging*, 37(6):1310–1321, 2017.

Jian Zhang and Bernard Ghanem. Ista-net: Interpretable optimization-inspired deep network for image compressive sensing. In *Proceedings of the IEEE conference on computer vision and pattern recognition*, pages 1828–1837, 2018.

Kai Zhang, Yawei Li, Wangmeng Zuo, Lei Zhang, Luc Van Gool, and Radu Timofte. Plug-and-play image restoration with deep denoiser prior. *IEEE Transactions on Pattern Analysis and Machine Intelligence*, 2021.

Hang Zhao, Orazio Gallo, Iuri Frosio, and Jan Kautz. Loss functions for image restoration with neural networks. *IEEE Transactions on computational imaging*, 3(1):47–57, 2016.